Elastic properties of $NiSi_2$, $CoSi_2$, and $FeSi_2$ by tight-binding calculations

Giovanna Malegori and Leo Miglio
Dipartimento di Fisica dell'Università di Milano, via Celoria 16, I-20133 Milano, Italy
(Received 4 March 1993)

In a semiempirical tight-binding scheme we calculate the total-energy curve for Ni, Fe, and Co disilicides in the CaF_2 structure. Agreement with recent linear muffin-tin-orbital, total-energy calculations, to which the band structure has been fitted at high-symmetry points of the Brillouin zone, is very satisfactory. Special attention has been devoted to the form of the phenomenological repulsive potential, in order to include the anharmonic contributions. Elastic constants, frozen-phonon frequencies, and cubic anharmonicities at the Γ point are also estimated, in quite good agreement with the existing experimental data.

I. INTRODUCTION

In the last ten years increasing interest has been devoted to the structural and electronic properties of transition-metal silicides[1-3] because of the possibility of employing these metallic materials for contacts in silicon-based devices or connections in integrated circuits. Actually, Ni and Co disilicides in the CaF_2 structure have a low resistivity (~ 50 and $\sim 20\ \mu\Omega$/cm, respectively[1]) and display good lattice matching to silicon (0.46% and 1.2%, respectively[4]), so that integration in silicon matrices could be possible with negligible strain and defect formation.

Very recently, sizable improvements have been achieved in the epitaxial growth of high-quality $NiSi_2$ and $CoSi_2$ films, both on top of the silicon substrate [ultrahigh-vacuum molecular-beam epitaxy (UHV MBE) (Ref. 4)] and inside it [molecular-beam allotaxy (MBA) (Ref. 5)]. These advancements have triggered, in turn, a renewed interest in measuring and calculating the most important physical properties of such materials. Several predictions of the electronic bands of $NiSi_2$ and $CoSi_2$ in the CaF_2 structure are present in the literature.[6] Still, the recent linear muffin-tin-orbital (LMTO) calculation by Lambrecht, Christensen, and Blöchl[7] is the only one where an estimate of the cohesive properties is also included.

No *ab initio* calculation of the elastic properties and phonon frequencies is currently available; nor do extensions to the silicon-silicide system seem at hand because of computer limitations. For this reason we present here a semiempirical tight-binding (TB) scheme, fitted onto the LMTO bands,[7] which reproduces very well the LMTO cohesion-energy curves as a function of the lattice parameter and provides an estimate of the elastic constants and the phonon frequencies (along with anharmonicities) at the Γ point, in satisfactory agreement with the existing experimental data. Moreover, this approach is easily transferable from one configuration to another, so that a comparison of the cohesive energies for different phases of $NiSi_2$ and $CoSi_2$ would be affordable, even in presence of the silicon substrate.

Very recently, iron disilicide ($FeSi_2$) has been actively studied both experimentally[8] and theoretically,[9] since, in the β phase, it displays a semiconductive gap. This configuration, 48 atoms in the unit cell, turns out to originate from a distortion of the simple CaF_2 phase, which is metallic and unstable in the bulk situation. However, the latest efforts in the UHV epitaxial growth of $FeSi_2$ (Ref. 10) indicate that the CaF_2 structure is obtained at low coverage on Si(111) substrates, along with a disordered phase in the same stoichiometry. Thus, we include the predictions for γ-$FeSi_2$ in our review of the elastic properties of metallic silicides in the CaF_2 structure. The tight-binding parameter have been consistently fitted to LMTO calculations,[9] but no comparison to the experimental elastic data has been to date possible. Here, again, total-energy calculations for β, CaF_2 and disordered phases would be very interesting and our method is likely to provide interesting information.[11]

II. TOTAL-ENERGY CALCULATIONS BY SEMIEMPIRICAL TIGHT BINDING

Following a standard procedure, we separate the total energy for valence electrons (e) and ion cores (c),

$$E_T(\mathbf{R}) = T_e + V_{ee} + V_{ec} + V_{cc} \ , \tag{1}$$

into a band-structure (BS) term and a repulsive (rep) part:

$$E_T(\mathbf{R}) = E_{\mathrm{BS}}(\mathbf{R}) + U_{\mathrm{rep}}(\mathbf{R}) \ , \tag{2}$$

where $\mathbf{R}$ stands for the whole set of core coordinates and

$$E_{\mathrm{BS}}(\mathbf{R}) \equiv 2 \sum_{n\mathbf{k}}^{E_F} E_n(\mathbf{k}) = T_e + V_{ec} + 2V_{ee} \ , \tag{3}$$

$$U_{\mathrm{rep}}(\mathbf{R}) \equiv \sum_{i<j}^{|\mathbf{R}_i - \mathbf{R}_j| < \bar{R}} f(|\mathbf{R}_i - \mathbf{R}_j|) = V_{cc} - V_{ee} \ . \tag{4}$$

The BS energy is just the summation of the one-particle

eigenstates up to the Fermi level E_F. These eigenstates are evaluated by a semiempirical tight-binding scheme which makes use of the two-center Slater-Koster parametrization.[12]

The TB matrix is fitted onto *ab initio* band-structure calculations at the equilibrium configuration $\{\mathbf{R}_0\}$, and a variation of atomic coordinates is included by scaling the two-center integrals with a power law of the interatomic distance d,[13]

$$H_{ll'm}(d)=H_{ll'm}(d_0)\left[\frac{d_0}{d}\right]^2,$$
$$H_{ldm}(d)=H_{ldm}(d_0)\left[\frac{d_0}{d}\right]^{3.5}, \tag{5}$$
$$H_{ddm}(d)=H_{ddm}(d_0)\left[\frac{d_0}{d}\right]^5,$$

where l and l' label s or p orbitals and m is the quantum number for the axial component of the angular momentum (σ, π, or δ). The on-site elements, on the contrary, are kept constant. Actually, they should be modified by a change in the overlap elements $S_{ll'm}$ and by charge-transfer effects (if any).[14] Still, the first one is included in U_{rep} and the second one is usually neglected in metallic silicides.

In fact, U_{rep} originates from the summation, up to first (or second) nearest neighbor, of the short-range potential terms $f(|\mathbf{R}_i-\mathbf{R}_j|)$, Eq. (4), which phenomenologically takes into account the nonorthogonality correction to the on-site TB elements and what remains of the near cancellation between the core-core and the electron-electron long-range interactions. In the common formulation for semiconductors, introduced by Chadi,[15] f is a quadratic polynomial:

$$f=f_0+U_1\left[\frac{|\mathbf{R}_i-\mathbf{R}_j|}{d_0}-1\right]+U_2\left[\frac{|\mathbf{R}_i-\mathbf{R}_j|}{d_0}-1\right]^2 \tag{6}$$

and Eq. (4) becomes

$$U_{\text{rep}}=U_0+U_1\sum_{i<j}^{|\mathbf{R}_i-\mathbf{R}_j|\le\bar{R}}\left[\frac{|\mathbf{R}_i-\mathbf{R}_j|}{d_0}-1\right]+U_2\sum_{i<j}^{|\mathbf{R}_i-\mathbf{R}_j|\le\bar{R}}\left[\frac{|\mathbf{R}_i-\mathbf{R}_j|}{d_0}-1\right]^2, \tag{7}$$

where $\bar{R}$ is usually the first-neighbor distance d_0, but the inclusion of second neighbors may be necessary, as in the case of CaF_2 silicides.

The repulsive energy, however, still depends parametrically on U_1 and U_2. The latter can be fixed by imposing the equilibrium and stability conditions at the experimental lattice spacing:

$$\left.\frac{\partial E_T}{\partial V}\right|_{V=V_0}\equiv\left.\frac{\partial E_{\text{BS}}}{\partial V}\right|_{V=V_0}+\left.\frac{\partial U_{\text{rep}}}{\partial V}\right|_{V=V_0}=0\ ; \tag{8}$$

$$\left.\frac{\partial^2 E_T}{\partial V^2}\right|_{V=V_0}\equiv\left.\frac{\partial^2 E_{\text{BS}}}{\partial V^2}\right|_{V=V_0}+\left.\frac{\partial^2 E_{\text{rep}}}{\partial V^2}\right|_{V=V_0}=-\left.\frac{\partial P}{\partial V}\right|_{V=V_0}=\frac{B}{V_0}\ . \tag{9}$$

Thus, we only need two external parameters plus knowledge of the TB elements at $\{\mathbf{R}_0\}$ (fitted or taken from universal laws[16]) to get a flexible expression of the total energy as a function of the atomic coordinates.

Actually, the repulsive potential of Eq. (6) includes just the harmonic terms, so that anharmonic effects are barely supplied by E_{BS}. Moreover, f is supposed to be rapidly decaying with interatomic distance, and the truncated polynomial is not consistent with such an ansatz. By considering the major contribution to U_{rep} in metallic systems to be due to nonorthogonality corrections of the basis set[14] and taking advantage of the similarity of our total-energy scheme to the Huggins-Mayer potential for alkali halides (band-structure attraction in place of the Madelung term[17]), we postulate an exponential form of f:

$$f=\phi\exp\left[-\alpha\left[\frac{|\mathbf{R}_i-\mathbf{R}_j|}{d_0}\right]\right], \tag{10}$$

so that

$$U_{\text{rep}}=\sum_{i<j}^{|\mathbf{R}_i-\mathbf{R}_j|\le\bar{R}}\phi\exp\left[-\alpha\left[\frac{|\mathbf{R}_i-\mathbf{R}_j|}{d_0}\right]\right], \tag{11}$$

which displays two parameters only (i.e., ϕ and α), as in the case of the harmonic potential. In fact, by expanding the exponential function around the equilibrium value, we obtain

$$U_0=N\phi e^{-\alpha},$$
$$U_1=-\alpha\phi e^{-\alpha},$$
$$U_2=\tfrac{1}{2}\alpha^2\phi e^{-\alpha},$$

where N is the coordination number and conditions (8) and (9) still hold. We will demonstrate in the following that this choice of the repulsive potential is important in order to get an accurate fit of the LMTO cohesion-energy curves for disilicides. This is true also in the case of silicon, which has been considered in a previous publication of ours.[18]

Calculations of the distortion energy corresponding to a lowering of the crystal symmetry are also possible. In fact, the elastic constants c_{11}, c_{12}, and c_{44} can be readily calculated in our scheme by considering the total-energy variation connected to the strain tensor $e_{\alpha\beta}$,[19]

$$\frac{\Delta E}{V_0}=\tfrac{1}{2}c_{11}(e_{xx}^2+e_{yy}^2+e_{zz}^2)+c_{12}(e_{xx}e_{yy}+e_{xx}e_{zz}+e_{zz}e_{yy})+\tfrac{1}{2}c_{44}(e_{xy}^2+e_{yz}^2+e_{zx}^2)\ . \tag{12}$$

For a suitable deformation of the macroscopic cell,

$$e_{xx}=0 ,$$
$$e_{yy}=\delta , \quad e_{\alpha\beta}=0 , \quad \alpha\neq\beta ,$$
$$e_{zz}=-\delta ,$$

which preserves the volume to first order in δ, we obtain the distortion-energy density

$$\frac{\Delta E}{V_0}=(c_{11}-c_{12})\delta^2 . \tag{13}$$

The bulk modulus, on the other hand, is readily expressed as a function of the elastic constant, by considering the energy-density variation (12) for an isotropic deformation $e_{xx}=e_{yy}=e_{zz}=(1/3)\delta$ and deriving it two times with respect to the volume [Eq. (9)]:

$$B=\tfrac{1}{3}(c_{11}+2c_{12}) . \tag{14}$$

Since the actual value of B is an input parameter in our frame, by Eqs. (13) and (14) we have

$$c_{11}=B+\frac{2\Delta E}{3V_0\delta^2} , \tag{15}$$

$$c_{12}=B-\frac{\Delta E}{3V_0\delta^2} . \tag{16}$$

For what concerns the determination of c_{44}, an internal strain is involved in the suitable deformation[20] and the calculation of the relaxation energy would be necessary. However, we can make a rough estimate of its value by taking the Keating expressions,[21] which substitutes the Cauchy relation for tetrahedrally coordinated crystals,

$$c_{44}=\frac{1}{2}\frac{(c_{11}-c_{12})(c_{11}+3c_{12})}{(c_{11}+c_{12})} . \tag{17}$$

This ansatz quite surprisingly provides a fair prediction of c_{44} also in the case of metallic $CoSi_2$, where comparison to experiments is possible. An important point, which will be addressed in the next section, is the accuracy in the determination of tiny ΔE [Eqs. (15) and (16)], stemming from the subtraction of the large quantities. This is a subtle problem, which deserves some care also in the determination of frozen-phonon frequencies and anharmonicities.

In principle, our total-energy scheme is suitable for the evaluation of any phonon energy, whenever the displacement pattern is known.[22] Here, we restrict our analysis to Γ-point vibrations, since displacements are readily estimated by symmetry arguments and no extension of the primitive unit cell is necessary. If we consider the distortion energy per cell, corresponding to optical modes with a displacement pattern $\{u_s\}$ in the $\langle 111\rangle$direction, we have (up to third order in u_s) (Ref. 23)

$$\Delta E^{\rm ph}=\sum_s \frac{1}{2}M_s\omega^2u_s^2+\sum_s 4\gamma\left[\frac{u_s}{\sqrt{3}}\right]^3+\mathcal{O}(u^4) , \tag{18}$$

where s labels the atoms inside the unit cell, ω is the phonon frequency, and γ is the cubic anharmonicity term, as defined by Wendel and Martin for silicon.[24]

The relative intensities of the core displacements u_s in the case of the polyatomic basis are determined by imposing the conservation of center-of-mass coordinates, so that the expression (18) becomes a single-variable polynomial to be equated with the distortion energy, as calculated by our method.

Estimations of ω and γ for the TO phonon in silicon are quite satisfactory,[18] especially for the latter, which turns out to be very well predicted by our exponential repulsive potential. Obviously, this frozen-phonon scheme does not allow for LO-TO splitting evaluation, since no macroscopic field contribution is here included.[22] However, this is not expected to be a relevant feature in the case of metallic silicides.

III. APPLICATION TO THE SILICIDES

The conventional cell of Ni-, Co-, and γ-$FeSi_2$ is displayed in Fig. 1. It corresponds to an fcc lattice with three atoms per unit cell:

$$M=a_0(0,0,0) ,$$
$$\mathrm{Si}_1=a_0(\tfrac{1}{4},\tfrac{1}{4},\tfrac{1}{4}) ,$$
$$\mathrm{Si}_2=a_0(-\tfrac{1}{4},-\tfrac{1}{4},-\tfrac{1}{4}) .$$

Therefore the metals (M) are tetrahedrally coordinated with respect to one silicon atom and M is inside a cubic cage of first-neighbor Si. The lattice parameter a_0 is 5.406 Å,[25] 5.365 Å (experimental values),[25] and 5.387 Å (*ab initio* prediction),[9] for Ni-, Co-, and γ-$FeSi_2$, respectively. We note that the interatomic distances are

$$d_{M\text{-Si}}=\frac{\sqrt{3}}{4}a_0 ,$$
$$d_{\text{Si-Si}}=\tfrac{1}{2}a_0 ,$$
$$d_{M\text{-}M}=\frac{1}{\sqrt{2}}a_0 ,$$

so that the first-neighbor (M-Si) and second-neighbor (Si-Si) distances are not very different, while $d_{M\text{-}M}$ is sensibly larger. After these crystallographic considerations, we decided to take advantage of a former TB calculation for $NiSi_2$ by Robertson[26] and to use the following basis set: sp^3 for Si and sp^3d^5 for M. Two-center integrals $H_{ll'm}$, involving the whole set are used for M-Si and Si-Si interactions, whereas $H_{pp\sigma}$ elements only are considered for M-M couplings. In Tables I, II, and III we report $H_{ll'm}$ and the on-site elements $E(l)$, as originated by our fitting to the LMTO bands at Γ and X.[7,9] We note that the $H_{ll'm}$ elements correctly scale from $NiSi_2$ to $CoSi_2$, ac-

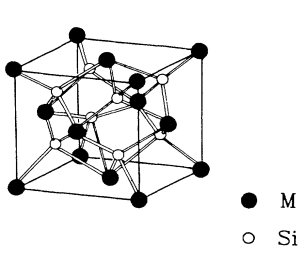

FIG. 1. Conventional cell of the CaF_2 structure.

TABLE I. TB parameters (eV) for $NiSi_2$ in the CaF_2 structure.

	d (Å)	$ss\sigma$	$sp\sigma$	$pp\sigma$	$pp\pi$	$sd\sigma$	$pd\sigma$	$pd\pi$
Ni-Si	2.34	−1.09	1.68	1.41	−0.63			
Si-Ni	2.34	−1.09	1.03	1.41	−0.63	−1.08	−0.95	0.58
Si-Si	2.70	−0.99	1.43	2.13	−0.86			
Ni-Ni	3.82			−0.21				
		$E(s)$	$E(p)$	$E(d)$				
Ni		2.44	8.18	−3.70				
Si		−5.68	1.06					

cording to the interatomic distance. $FeSi_2$, on the contrary, actually displays fitted elements which do not follow such a trend. We interpret this feature as a first indication that the CaF_2 structure is not the stable one for the bulk.

The electronic information enters our scheme through the total density of states (DOS), as integrated by a Green-function method over a mesh of about 800 points in the irreducible part of the Brillouin zone (BZ).[27] Our results are displayed in Fig. 2. They compare quite well with respect to the original LMTO DOS,[7,9] and the position of the Fermi level scales between $NiSi_2$ and $FeSi_2$ in the same way. For what concerns the latter, calculation of the Fermi level for any deformation of the equilibrium configuration has been performed. Our results for $NiSi_2$ in the case of isotropic compression and/or expansion is displayed in Fig. 3, where a decrease with respect to the lattice parameter is found, much steeper than the a^{-2} behavior of the free-electron model.

We have tested the validity of Andersen scaling laws $H_{ll'm} \propto (d_0/d)^{l+l'+1}$ (Ref. 28) in comparison to the Harrison ones, with no sizable differences in our calculations of the cohesion-energy curves. We have also tried to improve the fitting of $NiSi_2$, taking advantage of a larger set, which included d polarization orbitals for silicon, fitted onto different LMTO calculations.[29] The DOS at the equilibrium configuration is actually better reproduced. Still, total-energy calculations for the cohesion-energy curve pointed out that neither Harrison nor Andersen scaling rules are suitable for polarization orbitals. This is an interesting problem which deserves some more attention in the future.

For what concerns the repulsive potential f, we retained interactions up to Si-Si second neighbors only, in agreement with the structure of the TB matrix and with the larger distance occurring between M-M pairs. Therefore, the repulsive potential per unit cell for hydrostatic changes of volume is

$$U_{\rm rep}=8\phi\exp\left[-\alpha\left[\frac{d_{M\text{-Si}}}{d^0_{M\text{-SI}}}\right]\right]+6\phi\exp\left[-\alpha\left[\frac{d_{\text{Si-Si}}}{d^0_{M\text{-Si}}}\right]\right], \tag{19}$$

where the same two-body potential has been used for M-Si and Si-Si pairs. Since this term is mainly related to the overlap of atomic orbitals, we suspect that the parameters should be different if d orbitals are involved, in addition to s and p ones. Therefore our choice can be considered just a first approximation. On the other hand, as the Si-Si distance is not much larger than the M-Si one and only two input parameters are disposable in our model (a_0 and B), we decided to adopt expression (19), which turned out to give much better results than a first-neighbor summation only.

By considering the link between the isotropic changes of volume and the relative variation of the lattice parameter ($\varepsilon=a/a_0$) in the CaF_2 structure, conditions (8) and (9) become a pair of nonlinear equations

$$-\phi\alpha\left[e^{-\alpha}+\frac{\sqrt{3}}{2}e^{-2/\sqrt{3}\alpha}\right]=-\frac{1}{8}\left.\frac{\partial E_{\rm BS}}{\partial\varepsilon}\right|_{\epsilon=1}, \tag{20}$$

$$\phi\alpha^2(e^{-\alpha}+e^{-2\sqrt{3}\alpha})=-\frac{1}{8}\left.\frac{\partial^2 E_{\rm BS}}{\partial\varepsilon^2}\right|_{\epsilon=1}+\frac{9}{32}Ba_0^3, \tag{21}$$

which are solved by numerical methods. In particular, the first and second derivatives of $E_{\rm BS}$ have been estimat-

TABLE II. As in Table I for $CoSi_2$.

	d (Å)	$ss\sigma$	$sp\sigma$	$pp\sigma$	$pp\pi$	$sd\sigma$	$pd\sigma$	$pd\pi$
Co-Si	2.32	−1.12	1.71	1.42	−0.71			
Si-Co	2.32	−1.12	0.91	1.42	−0.71	−1.24	−1.06	0.68
Si-Si	2.68	−0.99	1.69	2.17	−0.86			
Co-Co	3.79			−0.22				
		$E(s)$	$E(p)$	$E(d)$				
Co		3.74	9.59	−1.61				
Si		−4.52	2.44					

TABLE III. As in Table I for $FeSi_2$.

	d (Å)	$ss\sigma$	$sp\sigma$	$pp\sigma$	$pp\pi$	$sd\sigma$	$pd\sigma$	$pd\pi$
Fe-Si	2.33	−1.31	1.38	1.57	−0.80			
Si-Fe	2.33	−1.31	1.16	1.57	−0.80	−1.28	−1.02	0.69
Si-Si	2.69	−0.88	1.45	2.55	−0.98			
Fe-Fe	3.81			−0.23				
		$E(s)$	$E(p)$	$E(d)$				
Fe		5.32	7.62	−0.93				
Si		−4.14	3.08					

ed in different ways, by analytic calculations, by numerical differentials, and by interpolating the numerical $E_{BS}(\varepsilon)$ curve with polynomials up to fourth order in $(\varepsilon-1)$ and with more physical scalings, such as

$$E_{BS}(\varepsilon)=A+D/\varepsilon^n . \quad (22)$$

All of them provided a satisfactory estimation of first and second derivatives, which agree within 1% and 5%, respectively. Equation (22), however, allows for a meaningful comparison of the exponent n among Ni-, Co-, and $FeSi_2$, and so we report in Table IV our results for A, D, n, ϕ, and α, along with the input parameters a_0, B.

IV. RESULTS

A. Cohesion-energy curves

Total energies for isotropic deformations are determined by summing up expressions (19) and (22), except for a constant-energy term, taking into account the free-atoms contribution. By adopting the parameters of Table IV we obtained the cohesion-energy curves displayed in Fig. 4 (solid lines). In the case of $NiSi_2$ and $CoSi_2$, comparison to LMTO data (open circles) is possible and very satisfactory, within the accuracy in reporting the graphical data of Ref. 7. As for the vertical energy rescaling mentioned above, the horizontal positions of our TB curves have been displaced for a_0 by 0.14 Å for $NiSi_2$ and 0.001 Å for $CoSi_2$ in order to let their minima superimpose to the LMTO predictions, which slightly overestimate the actual equilibrium values. By using a quadratic repulsive potential, as in the case of the Chadi model, the agreement is quite poor (dotted lines), since repulsive anharmonic terms are missing.

Such a good prediction of the cohesive-energy curves could be obtained also in the case of different crystalline phases, with no adjustment of the scaling laws, but for different repulsive terms for M-Si and Si-Si interactions. The transferability of our total-energy scheme has been recently tested for the case of $NiSi_2$ and $CoSi_2$ in the adamantane structure.[11]

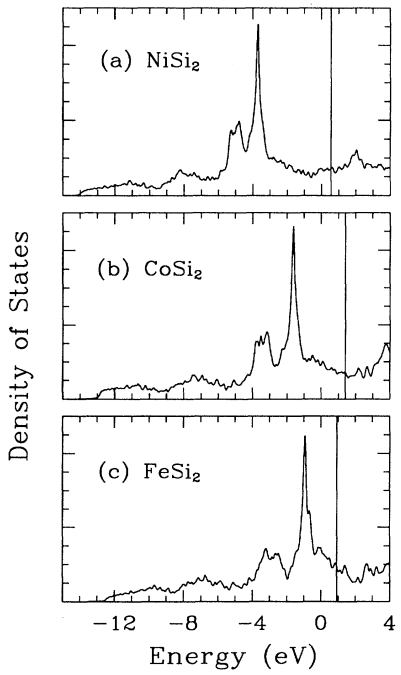

FIG. 2. Total DOS for (a) $NiSi_2$, (b) $CoSi_2$, (c) γ $FeSi_2$. The Fermi level is indicated by a vertical line.

B. Elastic constants

The elastic constants c_{11} and c_{12} are evaluated by Eqs. (15) and (16), with δ ranging from −0.05 to +0.05. Deformation of the unit cell corresponding to such a strain

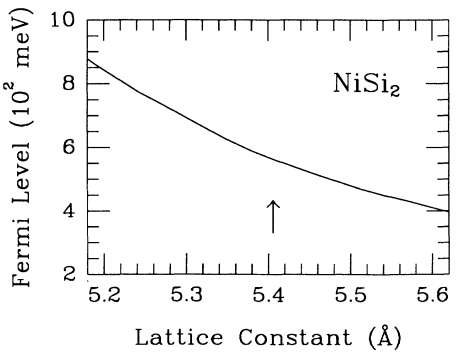

FIG. 3. Fermi level for $NiSi_2$, as a function of the lattice constant. The arrow indicates equilibrium value, as referring to Fig. 2.

TABLE IV. E_{BS} parameters A, D, and n [Eq. (22)], U_{rep} parameters ϕ and α [Eq. (11)], along with the input values for a_0 and B [experimental estimations (Refs. 25, 30, and 31) and theoretical predictions (Ref. 9 and 7)].

	a_0 (Å)	B (Mbar)	A (eV)	D (eV)	n	ϕ (keV)	α
$NiSi_2$	5.406[a]	1.60[b]	−59.86	−28.19	3.38	3.12	7.86
$CoSi_2$	5.365[a]	1.90[b,c]	−29.65	−31.70	3.49	4.00	7.97
		1.69[d]				2.77	7.56
$FeSi_2$	5.387[e]	2.06[e]	−16.12	−37.60	3.17	3.43	7.71

[a]Reference 25.
[b]Reference 7.
[c]Reference 30.
[d]Reference 31.
[e]Reference 9.

gives rise to small total-energy variations, so that integration on the irreducible part of the distorted BZ is performed with more than 1000 special points.[27] We fitted the distortion-energy curve $\Delta E(\delta)$ by a quartic polynomial, and we extracted the quadratic term. Table V reports the results for c_{11}, c_{12}, and c_{44} [estimated by Eq. (17)], along with a couple of experimental sets for $CoSi_2$, both by neutron-scattering measurements[30] and by the pulse-echo-overlap method.[31]

Obviously, our predictions depend on the B value, not only for what concerns Eqs. (15) and (16), but also from the very beginning, by Eq. (9). Thus, we compared the experimental data for $CoSi_2$ with consistent calculations

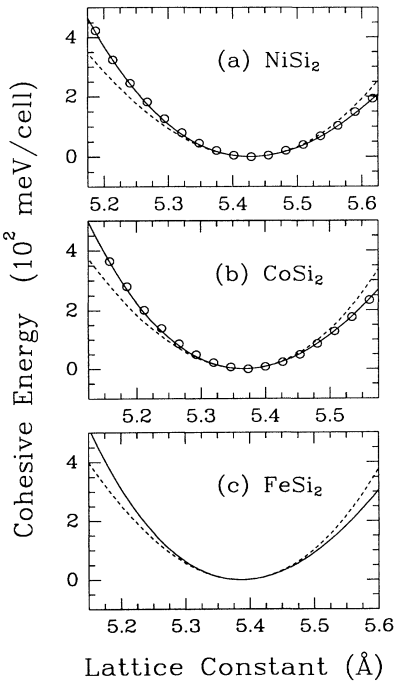

FIG. 4. Cohesion energy as a function of the lattice constant, calculated with U_{rep} in Eq. (7) (dashed line) and Eq. (11) (solid line): (a) $NiSi_2$, (b) $CoSi_2$, (c) γ $FeSi_2$. Circles are LMTO results (Ref. 7).

of ours and the agreement is rather good. For $NiSi_2$, experimental measurements are in progress. Still, preliminary estimations of $(c_{11}-c_{12})$ give us 0.57 Mbar,[32] in striking agreement with our estimation.

C. Phonon frequencies and anharmonicities

Optical vibrations at the Γ points involve (a) symmetric counterphase motion of the silicon atoms along $\langle 111 \rangle$ while the metal atom is at rest; and (b) counterphase $\langle 111 \rangle$ motion of the silicon atoms with respect to the metal, with a displacement ratio in such a way that the center of mass is at rest. The (a) mode is Raman active and lower in frequency; the (b) mode is IR active and higher in frequency.

We have calculated the tiny distortion energies corresponding to such phonons for Si displacements as large as 0.1 Å (both inward and outward[22]). Note that, because of the metallic character of the silicides we are studying, a large number of k points are considered. As an example, integration over the irreducible part of the distorted BZ is performed with about 3000 special points[27] in the case of $CoSi_2$. Figures 5 and 6 display our calculated distortion-energy curves for (a) and (b) displacement patterns, respectively (open squares). Quadratic and cubic terms in u_s, as required by Eq. (18), can be obtained by fitting our $\Delta E^{ph}(u_{Si})$ by a quartic polynomial (solid lines in Figs. 5 and 6): ν and γ are reported in Table VI. Our

TABLE V. Elastic constants (Mbar) calculated by the TB scheme, as compared to existing experimental data. The corresponding B value (Mbar) is also reported.

	B	$c_{11}-c_{12}$	c_{11}	c_{12}	c_{44}
$NiSi_2$ (TB)	1.60	0.58	1.99	1.41	0.53
$CoSi_2$ (TB)	1.90	0.74	2.39	1.65	0.67
$CoSi_2$ (expt.[a])	1.90	0.79	2.40	1.61	0.74
$CoSi_2$ (TB)	1.69	0.75	2.19	1.44	0.67
$CoSi_2$ (expt.[b])	1.69	0.88	2.28	1.40	0.83
$FeSi_2$ (TB)	2.06	0.87	2.64	1.77	0.78

[a]Reference 30.
[a]Reference 31.

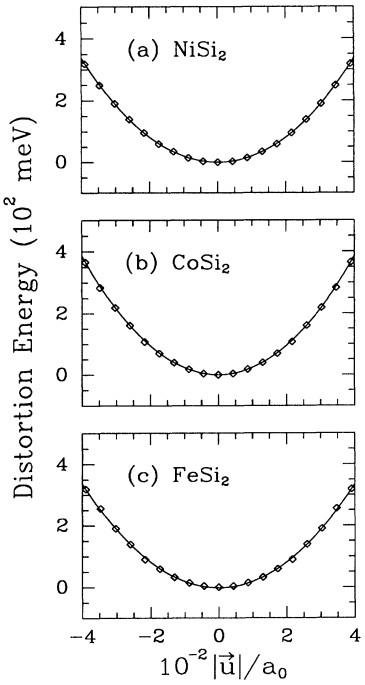

FIG. 5. Distortion energy for the displacement pattern corresponding to the IR-active mode at Γ: (a) $NiSi_2$, (b) $CoSi_2$, (c) γ $FeSi_2$. Open squares are the calculated values; solid lines are the fitting polynomials.

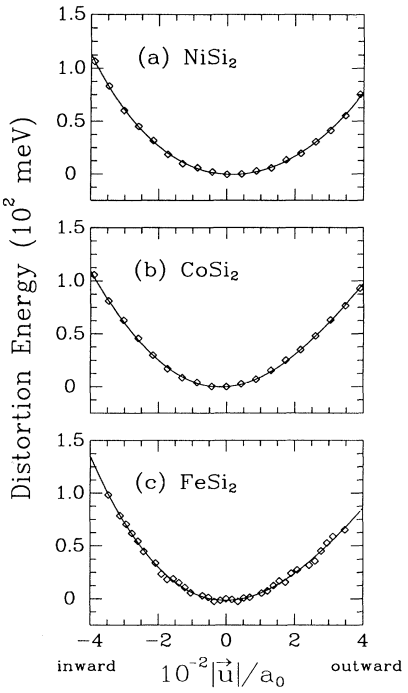

FIG. 6. As for Fig. 5 for what concerns the Raman-active mode at Γ. Note that for $FeSi_2$ this displacement pattern gives rise to a larger instability in the calculation of the distortion energy.

accuracy does not allow for the determination of quartic terms, which, however, are not usually reported in the literature, even for *ab initio* calculations.

The phonon frequency of the (a) mode in $CoSi_2$ can be compared to Raman data, where a single peak is observed at 267 cm^{-1}.[33] Our estimation is satisfactory, somehow higher than the experimental value, as for the case of silicon.[18] For $NiSi_2$, our frequencies can be compared to the Raman- and neutron-scattering measurements in disordered system.[3] Because of disorder activation, the Raman spectra display broadbands, representing the weighted phonon DOS. Comparison to our results is not as direct as in the case of sharp Raman peaks. Still, we can assign the (a) and (b) phonon frequencies to the Raman bands at 290 cm^{-1} and 372–392 cm^{-1}, respectively. Although the agreement is qualitatively satisfactory, we actually underestimate both (a) and (b) modes. Taking aside strain effects in the sample a residual indeterminancy in our predictions still remains from the fitting to the elastic modulus, so that optical phonons are very likely to be affected by a systematic error. Mazur and Pollman[34] have correctly suggested to fit a Γ-mode frequency, but this is possible just in the case of materials where a good wealth of experimental data is disposable.

For what concerns the anharmonic terms, the (a) mode displays a cubic contribution, which can be compared to the one for the optical mode in silicon, where $\gamma_{Si}=81.2$ $eV/Å^3$.[18] By taking into account that the bond deformation is double in silicon, $\gamma_{Si}/8 \simeq \gamma_{NiSi_2} \simeq \gamma_{CoSi_2}$ (see Table VI). For what concerns $FeSi_2$, on the contrary, we note that the anharmonic constant γ is more than 2 times larger, so that we may wonder whether this is another indication of the structural metastability of $FeSi_2$ in the CaF_2 structure. This is confirmed also by the larger instability in the calculation of the distortion energy corresponding to such a mode (see Fig. 6). Further investigations along these lines are in progress.

TABLE VI. Calculated phonon frequencies (cm^{-1}) and cubic anharmonicities ($eV/Å^3$). For what concerns $CoSi_2$, our calculations refer to the experimental estimation of B (Ref. 31).

	ν (Raman)	γ	ν (IR)
$NiSi_2$	263	9.90	373
$CoSi_2$	285	11.15	371
$FeSi_2$	310	25.52	355

ACKNOWLEDGMENTS

We thank Dr. H. von Känel and Dr. M. Mendik (ETH, Zurich) for helpful discussions on $FeSi_2$.

[1]S. P. Murarka, Ann. Rev. Mater. Sci. **13**, 117 (1983).
[2]C. Calandra, O. Bisi, and G. Ottaviani, Surf. Sci. Rep. **4**, 271 (1984).
[3]L. J. Chen and K. N. Tu, Mater. Sci. Rep. **6**, 53 (1991).
[4]H. von Känel, Mater. Sci. Rep. **8**, 193 (1992).
[5]S. Mantl and H. Bay, Appl. Phys. Lett. **61**, 267 (1992).
[6]W. Lee, D. M. Bylander, and L. Kleinman, Phys. Rev. B **32**, 6899 (1985); J. Tersoff and D. R. Hamman, *ibid.* **28**, 1168 (1983); D. M. Bylander, L. Kleinman, K. Mednick, and W. R. Grise, *ibid.* **26**, 6379 (1982); O. Bisi, L. W. Chiao, and K. N. Tu, *ibid.* **30**, 4664 (1984); J. Weaver, A. Franciosi, and W. L. Moruzzi, *ibid.* **29**, 3293 (1984).
[7]W. R. L. Lambrecht, N. E. Christensen, and P. Blöchl, Phys. Rev. B **36**, 2493 (1987).
[8]C. Giannini, S. Lagomasino, F. Scarinci, and P. Castrucci, Phys. Rev. B **45**, 8822 (1992); K. Lefki, P. Muret, E. Bustarret, N. Boutarek, R. Madar, J. Chevrier, J. Derrien, and M. Brunel, Solid State Commun. **80**, 791 (1991); J. Derrien, J. Chevrier, V. Le Thanh, and J. E. Mahan, Appl. Surf. Sci. **56-58**, 382 (1982); D. Gerthsen, K. Radermacher, Ch. Dieker, and S. Mantl, J. Appl. Phys. **71**, 3788 (1992).
[9]N. E. Christensen, Phys. Rev. B **42**, 7148 (1990).
[10]N. Onda, J. Henz, E. Müller, K. A. Mäder, and H. von Känel, Appl. Surf. Sci. **56-58**, 421 (1992).
[11]F. Tavazza, G. Malegori, and L. Miglio (unpublished).
[12]J. C. Slater and G. F. Koster, Phys. Rev. **94**, 1498 (1954).
[13]W. A. Harrison, *Electronic Structure and the Properties of Solids* (Freeman, San Francisco, 1980).
[14]J. A. Majewski and P. Vogl, in *The Structures of Binary Compounds,* edited by F. R. de Boer and D. G. Pettifor (North-Holland, Amsterdam, 1989), p. 287.
[15]D. J. Chadi, Phys. Rev. Lett. **41**, 1062 (1978); Phys. Rev. B **19**, 2074 (1979); **29**, 785 (1984).
[16]D. A. Papaconstantopoulos, *Handbook of the Band Structure of Elemental Solids* (Plenum, New York, 1986).
[17]M. L. Huggins and J. E. Mayer, J. Chem. Phys. **1**, 643 (1933).
[18]L. Miglio and G. Malegori, Nuovo Cimento D **15**, 467 (1993).
[19]C. Kittel, *Introduction to Solid State Physics* (Wiley, New York, 1987).
[20]D. J. Chadi and R. M. Martin, Solid State Commun. **19**, 643 (1976).
[21]P. N. Keating, Phys. Rev. **145**, B637 (1966).
[22]K. Kunc and R. M. Martin, in *Ab Initio Calculation of Phonon Spectra,* edited by J. T. Devreese *et al.* (Plenum, New York, 1983), p. 65.
[23]D. Vanderbilt, S. G. Louie, and M. L. Cohen, Phys. Rev. B **33**, 8740 (1986).
[24]H. Wendel and R. M. Martin, Phys. Rev. B **19**, 5251 (1979).
[25]W. B. Pearson, *Handbook of Lattice Spacing and Structures of Metals and Alloys* (Pergamon, New York, 1958).
[26]J. Robertson, J. Phys. C **18**, 947 (1985).
[27]H. J. Monkhorst and J. D. Pack, Phys. Rev. B **13**, 5188 (1976).
[28]O. K. Andersen, W. Klose, and H. Nohl, Phys. Rev. B **17**, 1209 (1978).
[29]F. Manghi, G. Guidetti, and O. Bisi, Appl. Surf. Sci. **56-58**, 416 (1992).
[30]L. Weiss, A. Y. Rumyantsev, and A. S. Ivanov, Phys. Status Solidi B **128**, k111 (1985).
[31]G. Guémin, M. Ignat, and O. Thomas, J. Appl. Phys. **68**, 6515 (1990).
[32]H. von Känel and M. Mendik (private communication).
[33]F. Li, N. Lustig, P. Klosowski, and J. S. Lammin, Phys. Rev. B **41**, 10 210 (1990).
[34]A. Mazur and J. Pollmann, Phys. Rev. B **39**, 5261 (1989); and (private communication).